Maximizing the Accuracy of QCT Cross Sections via Binning Methods

Jacob Ruben, Denuwan Vithanage, and Brian Stewart
Physics Department, Wesleyan University, Middletown CT, 06459

WESLEYAN UNIVERSITY

Introduction

- Quasiclassical trajectory (QCT) simulations model molecular collisions by solving classical equations of motion with quantum-like initial conditions. Dynamics are treated classically, while quantum effects like discrete vibrational and rotational states are accounted for during initialization and post-processing.
- We use quasiclassical trajectory (QCT) simulations and close-coupled (CC) quantum simulations to computationally determine cross sections.
- We use microscopic reversibility to ensure time reversal symmetry is upheld in our QCT simulations.
- For initially non-rotating molecules, QCT simulations poorly satisfy microreversibility when histogram binning is used.
- We propose binning methods for different situations to ensure micro reversibility is fulfilled while maintaining accuracy to quantum calculations.

Methods

Microscopic Reversibility

- Time reversal symmetry means our cross sections must satisfy microreversibility:

$$\frac{(2j_i+1)(E-\epsilon_i)\sigma_{i\to f}}{(2j_f+1)(E-\epsilon_f)\sigma_{f\to i}} = 1$$

Computational Methods

- We employ *ab initio* potential energy surfaces (PES) to model Li_2 - He, Li_2 - Ne, and Li_2 - Xe collisions.
- We use MOLSCAT, which solves the time-independent Schrödinger equation for non-reactive scattering given a PES. This essentially solves the problem exactly and is used as a comparison for our QCT simulation.
- Our QCT simulation transforms Hamilton's equations into action-angle coordinates, initializes quantum mechanically allowed vibrational and rotational actions (v_i,j_i) and integrates.
- Because the problem is solved classically, the final actions are continuous. They must then be discretized, or binned, into quantum mechanically allowed states, or quantum numbers v_f,j_f.
- We investigated both histogram and Gaussian binning, the latter at a variety of widths. Binning can be performed either asymmetrically, where the only the final actions are binned, or symmetrically, where the distribution of initial actions is binned in the same way as the final actions.

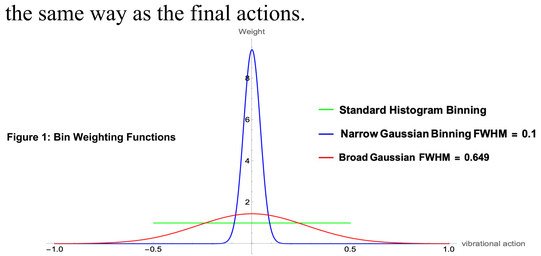

Figure 1: Bin Weighting Functions

Results

Microreversibility Results

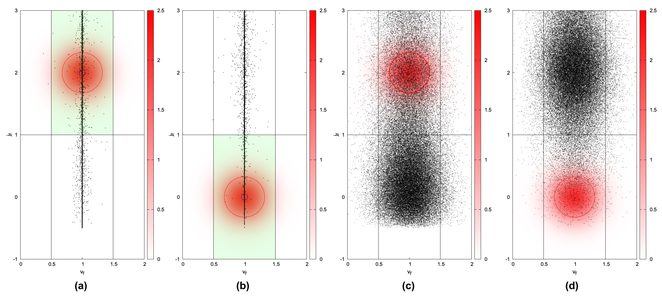

Figure 2: Final action distribution for v_i=1,j_i=0 → v_f=1,j_f=2 forward and reverse directions *(left: fixed initial state at v_i=1,j_i=0, right: gaussian distribution around initial state with FWHM 0.649, red circle: FWHM of gaussian weighting)*

Figures 2a and **2b** show final action distributions for v_i=1, j_i=0 → v_f=1, j_f=2 in the forward and reverse directions with initial actions fixed to quantum mechanically allowed values. The sharp cutoff at j = -0.5 is a necessary artifact of accounting for the rotational zero-point energy. The green shading indicates the region uniformly weighted by standard histogram binning, which clearly includes the large empty region in the elastic bin, leading to poor microreversibility ratios. **Figures 2c** and **2d** depict symmetrical binning, in which the initial actions follow a gaussian distribution with FWHM equal to the final binning method, here 0.649.

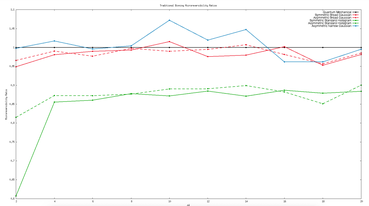

Figure 3: Microreversibility for basic binning types

Figure 3 compares microreversibility ratios for standard histogram binning and Gaussian binning with narrow (FWHM = 0.1) and broad (FWHM = 0.65) widths, applied symmetrically or asymmetrically. A Gaussian weighting clearly helps the sampling issue significantly.

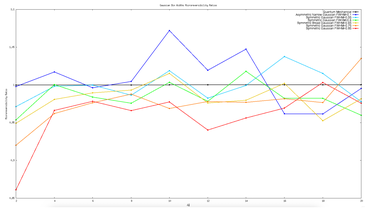

Figure 4: Microreversibility for various gaussian widths

Figure 4 shows how microreversibility varies with Gaussian FWHM between 0.1 and 0.85 — very broad Gaussians (e.g., FWHM = 0.85) worsen microreversibility by over-weighting empty regions in the elastic bin, similar to standard histogram.

Note: Both figures use Li_2-He collisions at 1027 cm^{-1} total energy, with the line at 1 being the computed quantum mechanical values obeying time reversal symmetry.

Rotationally Inelastic Results

For rotationally inelastic collisions, symmetric binning has better agreement with quantum cross sections. A wider Gaussian also outperforms both standard histogram and narrow Gaussian.

Helium

Figure 5 compares quantum with classical cross sections versus Δj for the binning methods introduced in **Figures 3** and **4**. **Figure 6** shows cross sections for v_i=1, j_i=0 → v_f=1, j_f=2 versus collision velocity. As expected, quantum effects dominate at low energies and converge toward classical results at higher energies.

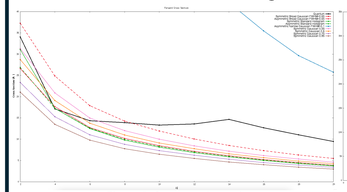

Figure 5: Cross section vs j_f

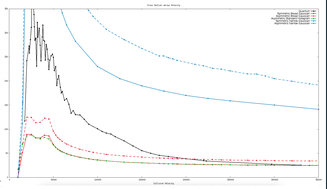

Figure 6: Cross section versus Collision velocity

Xenon

In **Figure 7** we compare cross sections as a function of final j for our main binning types. We can see that asymmetric standard histogram and symmetric Gaussian (FWHM 0.65) binning are very close to the quantum cross sections. In **Figure 8**, we compare quantum cross sections to various asymmetric Gaussian bin widths.

*Note that **Figure 7** is at 1527 cm^{-1} total energy while **Figure 8** is at 1027 cm^{-1}

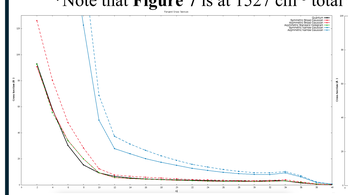

Figure 7

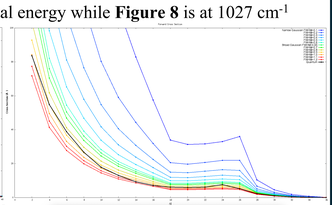

Figure 8

Figure 9 shows the cross section from v_i=1, j_i=0 → v_f=1, j_f=2 as a function of collision velcoity. It should be noted that for xenon, the low energy region shows much better agreement between quantum and classical cross sections.

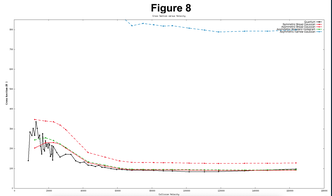

Figure 9

Comparing **Figure 5** with **Figures 7** and **8** we can see that quantum–classical agreement is generally better for helium than for xenon. We do not fully understand this trend yet. Our current hypothesis involves the relation between potential well depth and DeBroglie wavelength.

Vibrationally Inelastic Results

Unfortunately, the approach that works well for rotationally inelastic cross sections performs poorly for vibrationally inelastic collisions. As shown in **Figure 10a**, symmetric binning smears trajectories into vibrationally inelastic bins, drastically overestimating the cross sections. **Figure 10b** shows that using fixed initial states with a broad Gaussian bin (in red) has a similar issue: for wider Gaussians, the tails extend too far into the elastic bin, again overestimating the cross sections. This can be helped by truncating our Gaussian weighting function at three standard deviations from the mean and then renormalizing to make up for lost area.

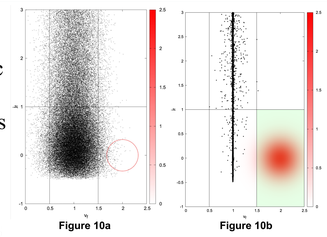

Figure 10a

Figure 10b

Xenon

Figure 11 compares quantum and classical cross section as a function of Δj for our standard binning methods. Symmetric broad Gaussian significantly overestimates the cross section, particularly at low j where trajectory density is highest. **Figure 12** shows cross sections for v_i=1, j_i=0 → v_f=0, j_f=20 versus collision velocity. Truncated broad Gaussian seems to have the best agreement with quantum cross sections here, with the untruncated broad Gaussian being so overestimated that it is barely visible here.

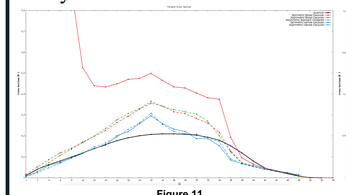

Figure 11

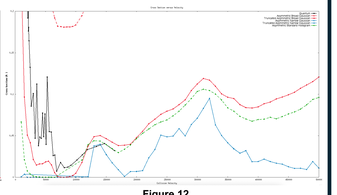

Figure 12

Helium

Figure 13 compares quantum and classical cross section as a function of Δj, while **Figure 14** shows cross sections for v_i=1, j_i=0 → v_f=0, j_f=20 versus collision velocity. In both cases, the quantum cross sections are extremely high, and we are currently unsure why. Classical binning behaves how we expect, but further investigation is necessary to understand the quantum mechanical behavior.

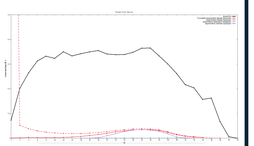

Figure 13

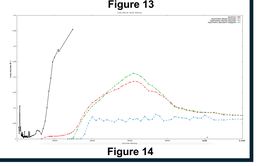

Figure 14

Conclusions

- For initially nonrotating molecules, standard histogram binning samples too large an area, and is strictly worse than Gaussian binning at satisfying microreversibility.
- There seems to be an optimal gaussian width, broader than the standard FWHM = 0.1, which avoids overestimating cross sections while remaining narrow enough to preventing oversampling similarly to standard histogram binning.
- Truncating the Gaussian weighting function seems to improve agreement with quantum results when investigating vibrationally inelastic collisions.

Future Work

- Analysis must be continued on Li_2-Ne to attempt to find a trend in the differences we see between Li_2-He and Li_2-Xe, whether that be due to mass, potential well depth and DeBroglie wavelength, etc.
- Higher energy quantum calculations need to be done to investigate convergence between quantum and classical results.
- We also plan to investigate the case of reactive collisions in the Li_2-Li system, where narrow gaussian binning is the norm.

References

1. Hutson, J. M. and S. Green, MOLSCAT computer code, version 14 (1994), distributed by Collaborative Computational Project No. 6 of the Engineering and Physical Sciences Research Council (UK).
2. McBane, G. C., "PMP Molscat", a parallel version of Molscat version 14 available at http://faculty.gvsu.edu/mcbaneg/pmpmolscat, Grand Valley State University (2005).
3. Smith, N., J. Chem. Phys. 85, 1987 (1986).
4. Bonnet, Int. Rev. Phys. Chem. 32, 171 (2013).